# Full-orbit and backward Monte Carlo simulation of runaway electrons

D. del-Castillo-Negrete
L. Carbajal
G. Zhang
D.A. Spong
L.R. Baylor
S.K. Seal

Oak Ridge National Laboratory

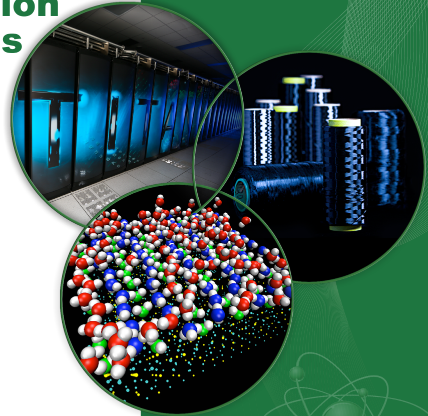

**Theory and simulations of Disruptions Workshop**

**PPPL**
**July 17-19, 2017**

# THE BIG PICTURE

- One of the main long term goals of the ORNL disruptions modeling and simulation team is the development of KORC (Kinetic Orbit Runaway Code): an integrated modeling capability for predictive studies of RE dynamics, generation, avoidance, and mitigation in ITER plasmas.
- KORC is designed as a modular code, with each module adding further physics and/or synthetic diagnostics.
- Particle tracking module: an accurate and efficient RE orbit integrator for general electric and magnetic fields in the presence of radiation damping.
    - KORC-GC: Guiding center orbit model
    - KORC-FO: Full orbit (6-dimensional) model.
- Synchrotron radiation synthetic diagnostic module: an accurate, efficient, and realistic diagnostic for radiation emission patterns and spectra taking into consideration full orbit and camera geometry effects.

## KORC (Kinetic Orbit Runaway Code)

- Collisions module: a Monte-Carlo based module for collisions with background plasma and impurities, and knock-on collisions.
- Radiative plasma cooling module: a continuum solver for a fluid model of impurity-induced plasma cooling and thermal quench.
- Conductive plasma cooling module: a Lagrangian-Green's function based solver for strongly anisotropic heat conduction in chaotic magnetic field during thermal quench.
- Electric field module: a continuum solver for the selfconsistent evolution of the electric field.

## KORC (Kinetic Orbit Runaway Code)

- Bremsstrahlung radiation synthetic diagnostic module: an accurate, efficient, and realistic model of bremsstrahlung radiation taking into consideration full geometric effects.
- MHD activity module: to incorporate MHD self-consistent effects.
- The methodology of the incorporation of the modules is guided by physics needs, and the implementation is guided by numerical methods accuracy and computing performance.
- Each module targets a specific physics problem with the expectation of getting new physics insights into the problem.
- Validation against experiments (DIII-D in particular) is a key element.

## RECENT RESULTS

- Full-orbit effects on RE dynamics [reported in last year's workshop].
  L. Carbajal, D. del-Castillo-Negrete, D. Spong, S. Seal, and L. Baylor, *Phys. of Plasmas* **24**, 042512 (2017).
- Synchrotron radiation: full-orbit effects and synthetic diagnostic [this talk].
  L. Carbajal and D. del-Castillo-Negrete, Submitted to *PPCF* (2017). arXiv:1707.03941.
- Backward Monte-Carlo method [this talk].
  G. Zhang and D. del-Castillo-Negrete, Submitted to *Phys. of Plasmas* (2017).
- RE dynamics with pellet suppression and instabilities (Alfven modes and whistler waves) [Don Spong presentation].

# KORC PARTICLE TRACKING MODULES WITH RADIATION DAMPING AND COLLISIONS DEVELOPED AND OPERATIONAL

## Guiding center orbit model

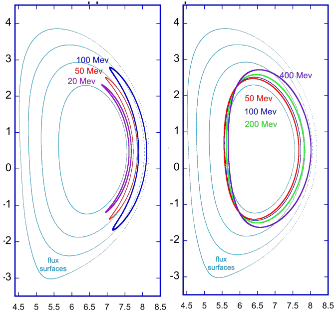


Trapped/passing orbits in ITER with 3D VMEC with field ripple and TBM perturbations

## Full orbit model

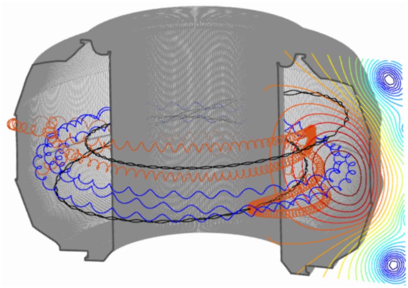

Trapped/passing orbits in DIII-D with JFIT fields

# ORBIT EFFECTS ON PITCH ANGLE DYNAMICS
## Collisionless pitch angle dispersion

- Even without collisions, RE exhibit pitch angle dispersion
- CPD results from full-orbit effects in spatially dependent magnetic fields
- CPD, which is ignored or treated approximately in reduced models, has a significant impact on synchrotron radiation

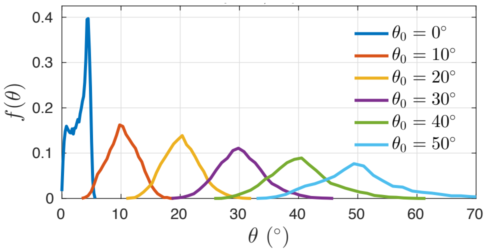


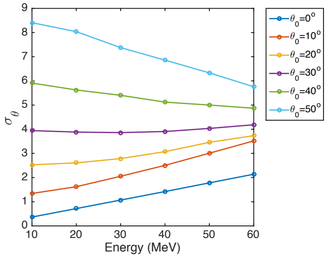

# ELECTRIC FIELD AND RADIATION DAMPING

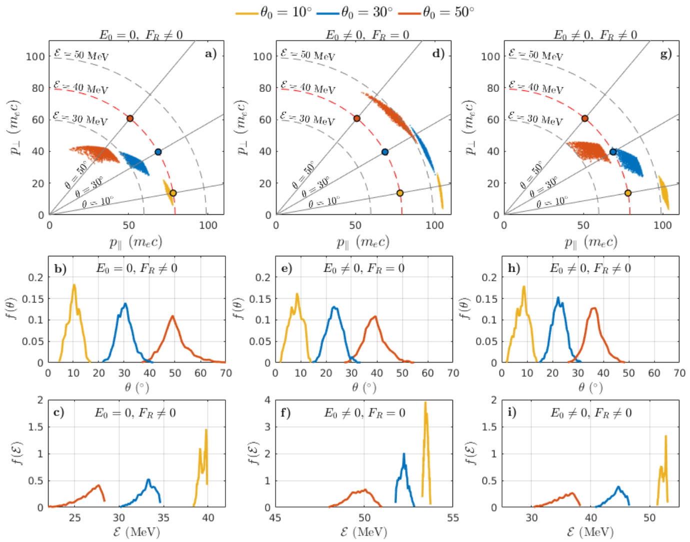


Summary of results of simulations of runaway electrons including synchrotron energy losses and a toroidal electric field.

## PITCH ANGLE EVOLUTION WITH COLLISIONS

DIII-D like magnetic field.

$t = 10\,\mathrm{ms}$

$E = 1\,\mathrm{V/m}$, $\mathcal{E}_0 = 30\mathrm{MeV}$, $\theta_0 = 5^o,\ 10^o,\ 15^o,$ and $20^o$.

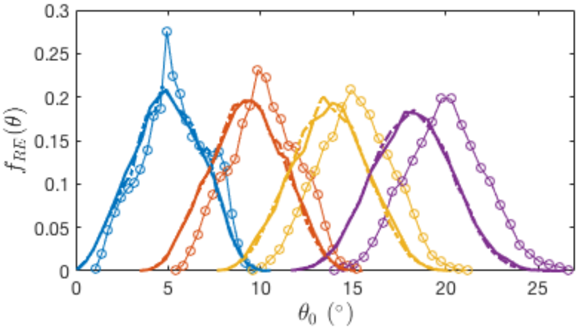


-o-o- No collisions no SR no E

— With collisions, no SR, and E    – – With collisions, SR, and E

# FULL ORBIT EFFECTS ON SYNCHROTRON RADIATION

- The total radiation power $P_T = \frac{e^2}{6\pi\epsilon_0 c^3}\gamma^4 v^4 \kappa^2$ depends on the geometry of the orbit through the curvature
- Approximating $\kappa$ assuming $\theta$ and/or $B$ constant (as done in reduced models) can introduce significant errors in $P_T$

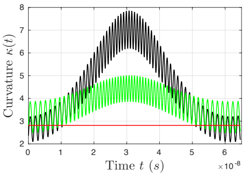


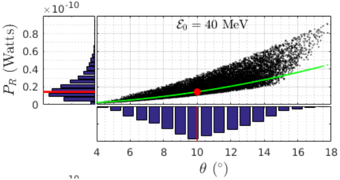


DIII-D-like

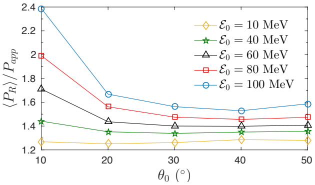


ITER-like

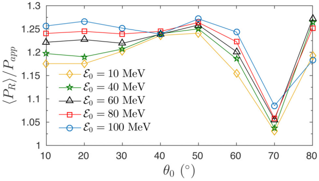

# FULL ORBIT EFFECTS ON SYNCHROTRON RADIATION

$$P(\lambda) = \frac{4\pi}{\sqrt{3}} c e^2 \left( \frac{mc^2}{\mathcal{E}} \right)^2 \frac{1}{\lambda} \int_{\lambda_c/\lambda}^{\infty} K_{5/3}(\eta)\, d\eta \qquad \lambda_c = \frac{4\pi}{3\kappa} \left( \frac{mc^2}{\mathcal{E}} \right)^2$$

Ignoring orbit dependence of $\kappa$ can lead to inaccuracies in $P(\lambda)$

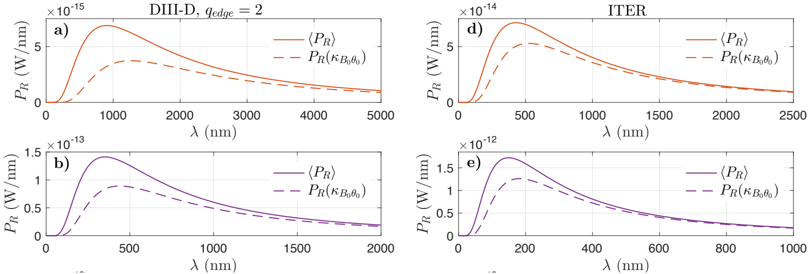


$\mathcal{E} = 40\text{MeV}$; $\theta_0 = 20^o$ and $\theta_0 = 30^o$.

# SYNCHROTRON RADIATION ROUTINELY MEASURED TO INFER RE INFORMATION

This motivates the need of accurate synthetic diagnostics that incorporate full-orbit effects

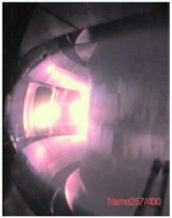


Visible camera in EAST [Y. Shi et al. Rev. Sci. Instrum. **81,** 033506 (2010)].

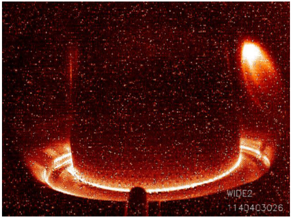


Visible camera in C-Mod [A. Tinguely et al. APS DPP 2016].

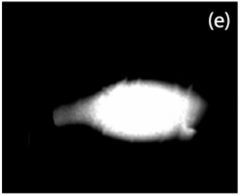


IR camera in TEXTOR [K. Wongrach et al. Nucl. Fusion **54,** 043011 (2014)].

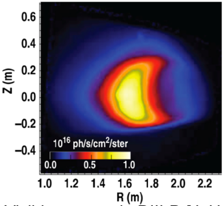


Visible camera in DIII-D [J. H. Yu et al. PoP **20**, 042113 (2013)].

# SYNCHROTRON SPATIAL EMISSION

- The modeling of measured 2D synchrotron images requires the computation of the power spectra as function of the observation vector $\hat{\mathbf{n}}$

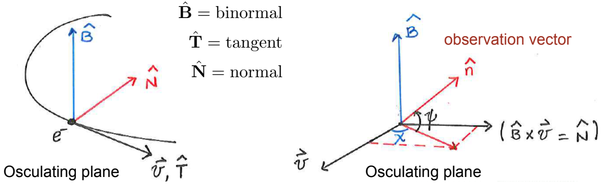


$$P(\lambda,\psi,\chi) = -\frac{4\pi c e^2}{\sqrt{3}\lambda^4\kappa}\left(\frac{1}{\gamma^2}+\psi^2\right)^2\left[\frac{\gamma^2\psi^2}{1+\gamma^2\psi^2}K_{1/3}(\zeta)\cos\Omega - \right.$$
$$\left. -\frac{1}{2}K_{1/3}(\zeta)\left(1+z^2\right)\cos\Omega + K_{2/3}(\zeta) z\sin\Omega\right]$$

where

$$\zeta = \frac{2\pi}{3\lambda\kappa}\left(\frac{1}{\gamma^2}+\psi^2\right)^{3/2}, \qquad z = \frac{\gamma\chi}{\sqrt{1+\gamma^2\psi^2}}, \qquad \Omega = \frac{3}{2}\zeta\left(z+\frac{1}{3}z^3\right)$$

# KORC SYNCHROTRON EMISSION SYNTHETIC DIAGNOSTIC

The recently developed diagnostic in KORC computes $P(\lambda, \psi, \chi)$ using the full-orbit information of large ensembles of RE incorporating the basic camera geometry

- We calculate the **SR spatial distribution on the poloidal plane**, as well as the **SR as seen by a camera** placed at the outer midplane plasma.

- We use two models for the angular distribution of the SR for computing the radiation seen by a camera:

  I. We use the full angular and spectral distribution $P_R(\lambda, \psi, \chi)$ .

  II. We assume that the radiation intensity is given by $P_R(\lambda)$ , and is emitted isotropically within a circular cone (natural opening angle) [K. Wongrach et al. Nucl. Fusion **54**, 043011 (2014)].

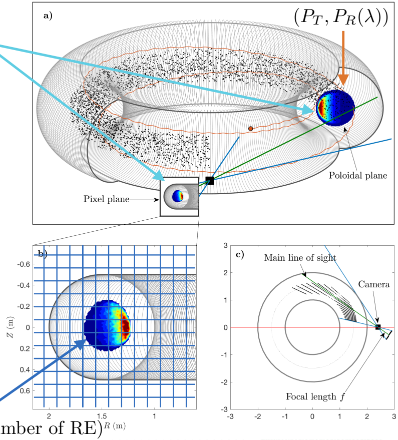


For each pixel we measure: $(P_R(\lambda, \psi, \chi), \text{Number of RE})$

# SPATIAL DISTRIBUTION OF RADIATION POWER IN THE **POLOIDAL PLANE**

## Mono-energetic and mono-pitch initial RE distribution function

$E = 30 MeV \;\; \theta = 10^0$

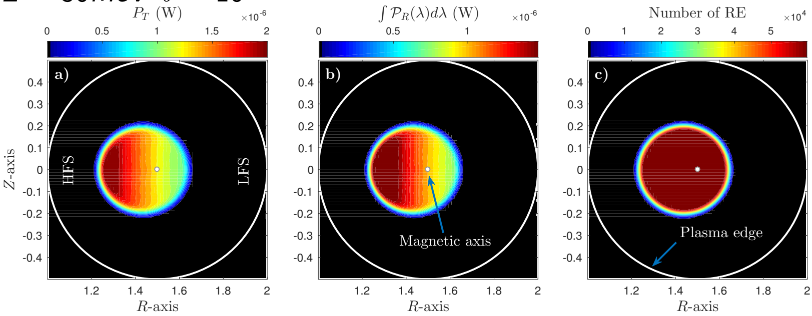


a) Total synchrotron radiated power. b) Power integrated over $\lambda \in (10^2, 10^4)\mathrm{nm}$. c) Spatial distribution of RE.

# SPATIAL DISTRIBUTION OF RADIATION POWER AS **MEASURED BY THE CAMERA**

Mono-energetic and mono-pitch initial RE distribution function

$E = 30 MeV$ and $\theta = 5^0, 10^0, 20^0$.

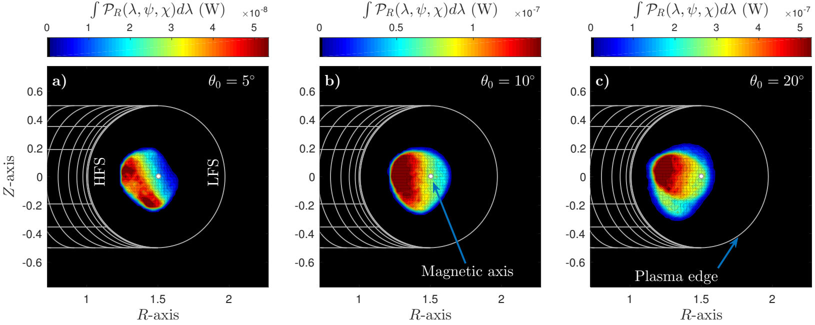


A transition from a crescent shape to an ellipse shape is observed as the pitch angle increases.

# SYNCHROTRON SPECTRA AS **MEASURED BY THE CAMERA**

Mono-energetic and mono-pitch initial RE distribution function

$E = 30MeV$ and $\theta = 5^0,\ 10^0,\ 20^0$.

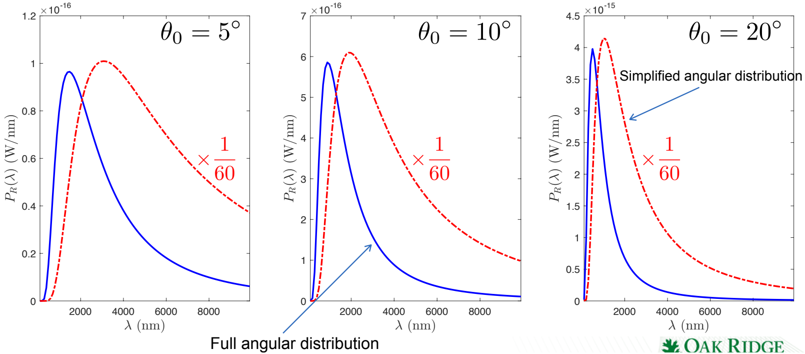


Oversimplification of the angular dependence overestimates the spectra and shifts the maximum.

# SYNCHROTRON SPECTRA ON **POLOIDAL PLANE**

## Avalanche type initial RE distribution function

$$f_{RE}(p,\eta) = \frac{\hat{E}p}{2\pi C_z \eta} \exp\left(-\frac{p\eta}{C_z} - \frac{\hat{E}p}{2\eta}(1-\eta^2)\right)$$

Left panels: Orbit-induced pitch angel dispersion modifies the RE pdf.
(a) Model distribution; (b) Modified distribution due to full-orbit effects.

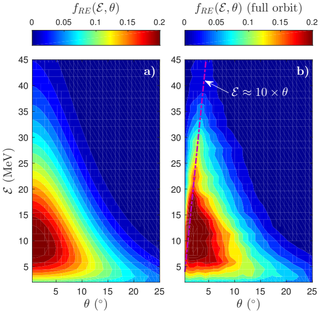


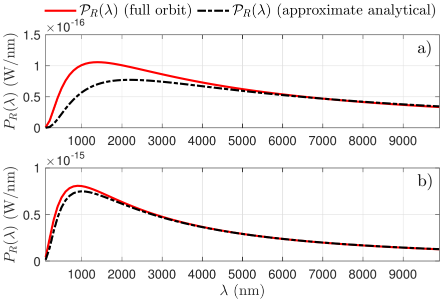


Right panels: Not including full-orbit effects underestimates the spectra.
(a) $Z_{eff} = 1$, (b) $Z_{eff} = 10$.

# SYNCHROTRON SPECTRA AS **MEASURED BY THE CAMERA**

## Avalanche type RE distribution function

$$f_{RE}(p,\eta) = \frac{\hat{E}p}{2\pi C_z \eta} \exp\left(-\frac{p\eta}{C_z} - \frac{\hat{E}p}{2\eta}(1-\eta^2)\right)$$

Left panels: Orbit-induced pitch angel dispersion modifies the RE pdf. (a) Model distribution; (b) Modified distribution due to full-orbit effects.

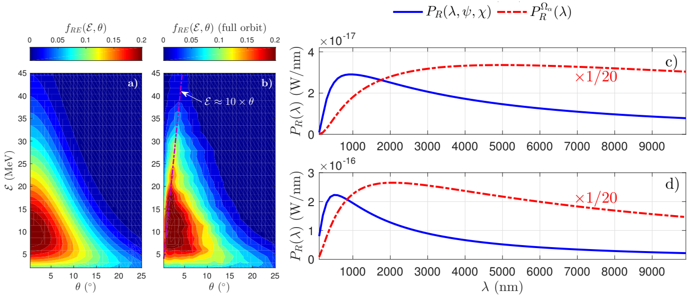


Right panels: Not including full angular dependence of the synchrotron emission and full-orbit effects significantly overestimates the spectra. (a) $Z_{eff} = 1$, (b) $Z_{eff} = 10$.

## BACKWARD MONTE CARLO METHOD

To illustrate the method we will use the simple 2-D Fokker-Planck model:

$$\frac{\partial f}{\partial t} = \mathcal{F} + \mathcal{C} + \mathcal{R}\,,$$

- Electric field acceleration:

$$\mathcal{F} = -E\left[\frac{\xi}{p^2}\frac{\partial}{\partial p}\left(p^2 f\right) + \frac{\partial}{\partial \xi}\left(\frac{1-\xi^2}{p} f\right)\right]$$

- Collisions operator:

$$\mathcal{C} = \frac{1}{p^2}\frac{\partial}{\partial p}\left[\left(1+p^2\right) f\right] + \frac{\nu_c}{2}\frac{\partial}{\partial \xi}\left[\left(1-\xi^2\right)\frac{\partial f}{\partial \xi}\right]$$

  with $\nu_c = (Z+1)\sqrt{1+p^2}/p^3$.

- Synchrotron radiation reaction force:

$$\mathcal{R} = \frac{1}{\tau}\left\{\frac{1}{p^2}\frac{\partial}{\partial p}\left[p^3\gamma\left(1-\xi^2\right) f\right] - \frac{\partial}{\partial \xi}\left[\frac{1}{\gamma}\xi\left(1-\xi^2\right) f\right]\right\}.$$

## STOCHASTIC DIFFERENTIAL EQUATION MODEL

$\theta =$pitch angle, $\xi = \cos\theta$
$p =$ magnitud of relativistic momentum.

$$dp_t = b_1(p_t, \xi_t)\, dt,$$
$$d\xi_t = b_2(p_t, \xi_t)\, dt + \sigma(p_t, \xi_t)\, dW_t,$$

where

$$b_1 = E\xi - \frac{\gamma p}{\tau}\left(1 - \xi^2\right) - \frac{1 + p^2}{p^2},$$
$$b_2 = \frac{E\left(1 - \xi^2\right)}{p} + \frac{\xi\left(1 - \xi^2\right)}{\tau\gamma} - \xi\nu_c$$
$$\sigma = \sqrt{\nu_c\,(1 - \xi^2)}, \qquad \tau = \tau_r/\tau_c$$

$\tau_c = m_e c/(E_c e)$ and $\tau_r = 6\pi\epsilon_0 m_e^3 c^3/(e^4 B^2)$.
$W_t$ is the standard Wiener process (Brownian motion) according to which the increments $dW_t$ are drawn from a Gaussian distribution with zero mean and variance equal to $dt$.

## PROBLEM FORMULATION

- What is the probability, $P_{\mathrm{RE}}$, that an electron with coordinates $(p, \xi)$ will runaway at, or before, a prescribed time?
- More formally: for $(t, p, \xi) \in [0, T] \times [p_{\min}, p_*] \times [-1, 1]$, where $p_{\min}$ is a lower momentum boundary, $P_{\mathrm{RE}}(t, p, \xi)$, is defined as the probability that an electron located at $(p, \xi)$ at $t_0 = 0$ will acquire a momentum $p_*$ on, or before, $t > 0$.

Given $f(t, p_t, \xi_t \,|\, p, \xi)$,

$$P_{\mathrm{RE}} = \mathbb{E}[\chi(p_t, \xi_t) \,|\, p_0 = p, \xi_0 = \xi] = \int_{\mathbb{R}^2} \chi(p_t, \xi_t) f(t, p_t, \xi_t \,|\, p, \xi) \, dp_t \, d\xi_t$$

where

$$\chi(p_t, \xi_t) = \begin{cases} 1, & \text{if } \; p_t \geq p_*, \\ 0, & \text{otherwise,} \end{cases}$$

indicates if a realization $(p_t, \xi_t)$ of the SDEs is a runaway path.

## DIRECT AND ADJOINT METHOD TO COMPUTE $P_{\mathrm{RE}}$

- Direct, "brute-force", MC method: simulate a very large number of paths, $(p_t, \xi_t)$, by solving the SDEs with initial condition $(p_0, \xi_0) = (p, \xi)$, and use the paths to approximate the expectation.
- Simple but very inefficient due to the slow convergence of the MC sampling, and the need to generate new set of paths at each point in phase space.
- Adjoint method [Liu, et al, 2016, 2017] get $P = P_{\mathrm{RE}}(T - t, p, \xi)$ for $(t, p, \xi) \in [0, T] \times [p_{\min}, p_*] \times [-1, 1]$ by solving the terminal value problem

$$\begin{cases} \dfrac{\partial P}{\partial t} + b_1 \dfrac{\partial P}{\partial p} + b_2 \dfrac{\partial P}{\partial \xi} + \dfrac{\sigma^2}{2} \dfrac{\partial^2 P}{\partial \xi^2} = 0, \\ P(T, p, \xi) = \chi(p, \xi), \end{cases}$$

# BACKWARD MONTE CARLO (BMC) METHOD

The key idea of the BMC method is to compute $P(t, p, \xi)$ directly from the Feynman-Kac formula giving the probability that a particle at $(p, \xi)$ at time $t$, will runaway at a time $\leq T$

$$P(t, p, \xi) = \mathbb{E}[\chi(p_T, \xi_T) \,|\, p_t = p, \xi_t = \xi]$$

where $\chi(p_T, \xi_T) = P(T, p_T, \xi_T)$.

- Introduce a uniform partition of the time interval $[0, T]$,

$$\mathcal{T} = \{0 = t_0 < t_1 < \cdots < t_N = T\},$$

- Within the time interval $[t_n, t_{n+1}]$,

$$P(t_n, p, \xi) = \mathbb{E}\left[P(t_{n+1}, p_{t_{n+1}}, \xi_{t_{n+1}}) \mid p_{t_n} = p, \xi_{t_n} = \xi\right].$$

- For small $\Delta t = t_{n+1} - t_n$

$$\begin{aligned} p_{t_{n+1}} &= p_{t_n} + b_1(p_{t_n}, \xi)\,\Delta t \\ \xi_{t_{n+1}} &= \xi_{t_n} + b_2(p_{t_n}, \xi_{t_n})\,\Delta t + \sigma(p_{t_n}, \xi_{t_n})\,\Delta W, \end{aligned}$$

# BACKWARD MONTE CARLO (BMC) METHOD

Within $(t_n, t_{n+1})$, the expectation can be approximated as

$$P(t_n, p, \xi) \approx \int_{\mathbb{R}} P\left(t_{n+1}, p + b_1 \Delta t, \xi + b_2 \Delta t + \sigma x\right) \; \frac{e^{-\frac{1}{2}\frac{x^2}{\Delta t}}}{\sqrt{2\pi \Delta t}} dx \,,$$

That is, the computation of $P(t_n, p, \xi)$ knowing $P(t_{n+1}, p, \xi)$ is reduced to the evaluation of an integral that can be efficiently computed using the Gauss-Hermite quadrature rule

$$P(t_n, p, \xi) \approx \sum_{m=1}^{M} w_m P(t_{n+1}, p^{\mathrm{GH}}, \xi_m^{\mathrm{GH}}), \tag{1}$$

where $M =$ number of quadrature points, $w_m =$ weights,

$$\xi_m^{\mathrm{GH}} = \xi + b_2(p, \xi)\Delta t + \sigma(p, \xi)\sqrt{2\Delta t}\; q_m,$$

and $\{q_m\}_{m=1}^{M}$ is the standard Gauss-Hermite abscissa.

# COMPARISON BETWEEN BMC AND DIRECT MC

Pitch angle $\theta = 10^\circ$ and $T = 1.6$.

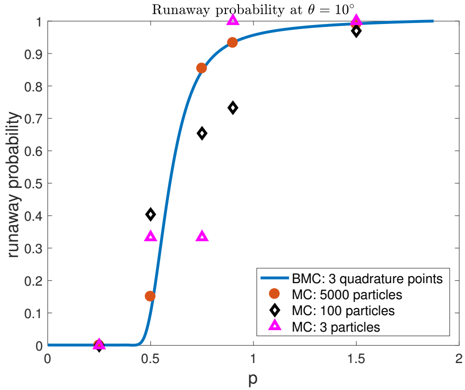

# SCALING OF BMC METHOD RELATIVE ERROR

$(p, \theta) = (0.7, 10^\circ), (0.7, 45^\circ), (0.7, 80^\circ)$ and $T = 1.6$.

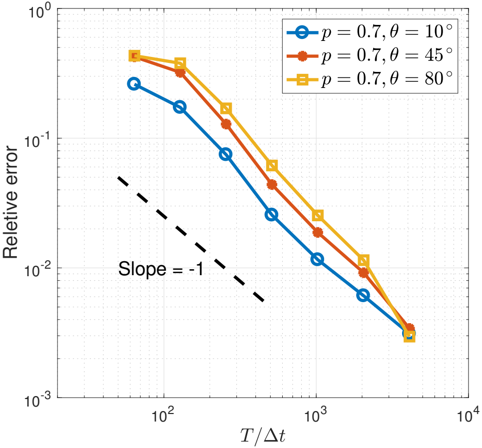

# TIME EVOLUTION OF PROBABILITY OF RUNAWAY $P_{RE}$

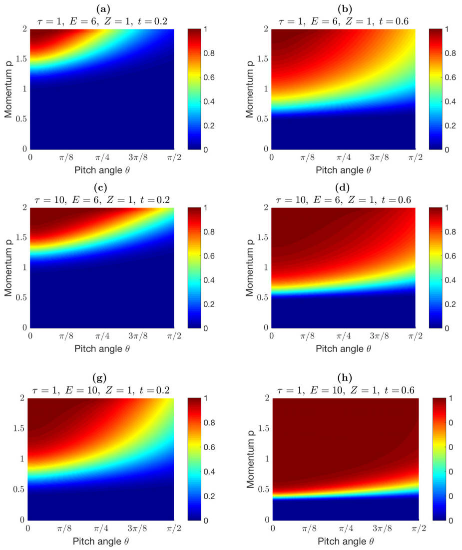


Radiation reaction force $\sim 1/\tau$, collisions $\sim Z$, acceleration $\sim E$.

# STEADY STATE (TIME ASYMPTOTIC) PROBABILITY OF RUNAWAY

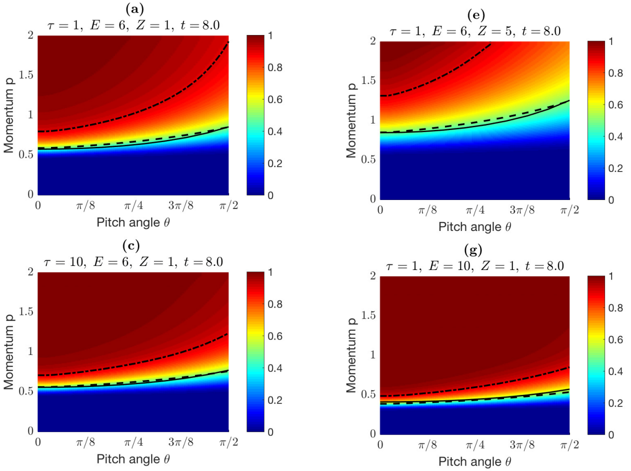


"- · - ·" $P_{\mathrm{RE}} = 0.9$, "- - -" $P_{\mathrm{RE}} = 0.5$, and "—" 0-D particle model.
Radiation reaction force $\sim 1/\tau$, collisions $\sim Z$, acceleration $\sim E$.

# EXPECTED RUNAWAY TIME

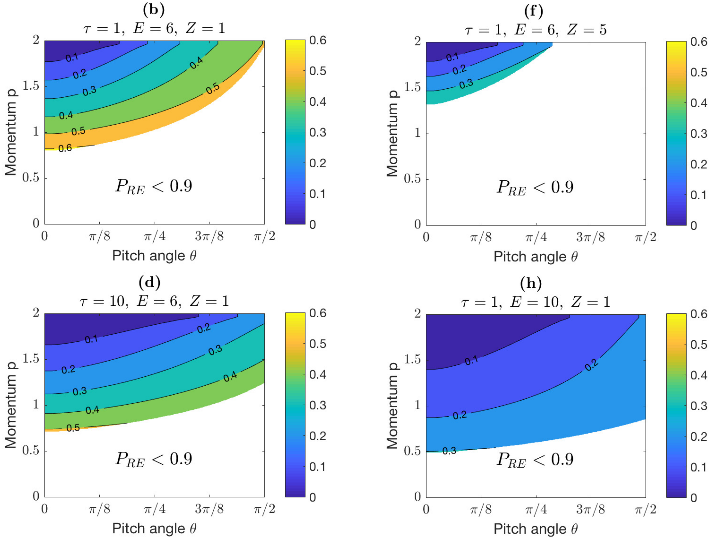

# EXPECTED LOSS TIME

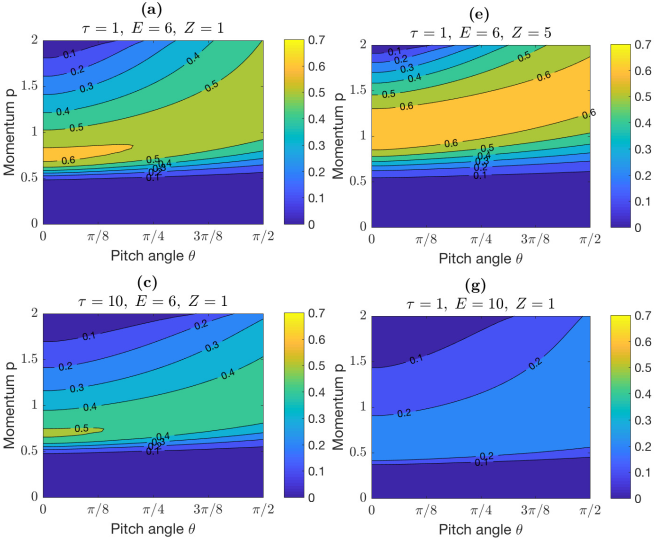

# DEPENDENCE OF RESULTS ON RUNAWAY BOUNDARY $p^*$

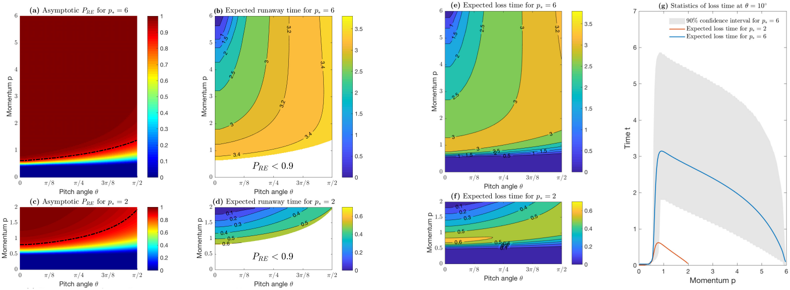


(a) & (c) Asymptotic $P_{\mathrm{RE}}$ for $p_* = 6$ and $p_* = 2$

(b) & (d) Expected runaway time for $p_* = 6$ and $p_* = 2$

(e) & (f) Expected loss time for $p_* = 6$ and $p_* = 2$

(g) Mean and 90% confidence interval of loss time for $\theta = 10^\circ$

# PRODUCTION RATE

$$\gamma = \frac{N_{\mathrm{RE}}(t)}{N} = \int_0^\infty dp \int_{-1}^{1} d\xi\, f(p,\xi) P_{\mathrm{RE}}(t,p,\xi)\,.$$

For a Maxwellian distribution

$$\gamma(t) = \frac{2}{\sqrt{\pi}\delta^3} \int_0^{p_*} dp\, e^{-(p/\delta)^2} p^2 \int_{-1}^{1} d\xi\, P_{\mathrm{RE}}(t,p,\xi) \; + \gamma_\infty\,,$$

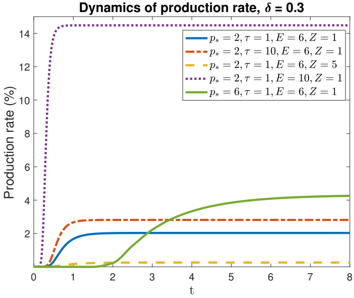


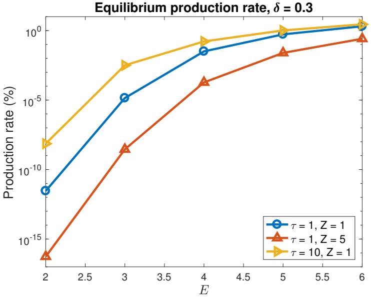


Radiation reaction force $\sim 1/\tau$, collisions $\sim Z$, acceleration $\sim E$.

# CONCLUSIONS

- The serious threat posed by disruptions in general, and runaway electrons in particular, to ITER calls for the development of advanced modeling and simulation efforts.
- Reduced models need to be complemented by detailed quantitative modeling that do not rely on restrictive assumptions.
- Of particular interest is the incorporation of space-dependent geometric effect.
- The ORNL program target these efforts, focussing on the development of KORC (Kinetic Orbit Runaway electrons Code), and backward Monte-Carlo methods.

# CONCLUSIONS

- KORC is designed as a modular code, with each module adding different physics and diagnostics.
- Current modules include full-orbit relativistic integrator for RE in the presence of general 3-D electric and magnetic (integrable or chaotic) fields with radiation damping and collisions.
- In parallel to the full-orbit module, we have also developed a guiding center relativistic integrator for RE (KORC-GC).
- Most recently we have added a synchrotron synthetic diagnostic.

## CONCLUSIONS

- **Orbit effects on synchrotron radiation (SR)**:
  - Collisionless (orbit-induced) pitch angle scattering has a direct effect on the RE distribution function and thus on SR.
  - Orbit-averaged 2-D phase space models underestimate SR power and shift the spectra.
- **SR synthetic diagnostic**:
  - Incorporates full-orbit information, camera geometry, and full-angular dependence of radiation
  - SR distribution on "camera plane" dependent on angular distribution of radiation and not trivially related to distribution on poloidal plane.
  - Oversimplification of the angular distribution of SR overestimates the intensity of the radiation as measured by a camera.

# CONCLUSIONS

- **Backward Monte Carlo Method**:
  - Based on the direct solution of time-discretized Feynman-Kac formula using Gauss-Hermite quadrature methods.
  - Accurate, efficient, and unconditional stable method.
  - Used to compute the time-dependent probability of runaway, expected runaway time, expected loss time, and production rate.
  - Extension to high-dimensional cases (i.e., beyond 2-D phase space) not a significant challenge exploiting sparse quadrature rules.
- **Modeling and simulation of impurity-based RE suppression**: [Don Spong presentation].